Forward-Masked Frequency Selectivity Improvements in Simulated and Actual Cochlear Implant Users Using a Preprocessing Algorithm

Florian Langner[1,2,3] and Tim Jürgens[1,2]

Abstract

Frequency selectivity can be quantified using masking paradigms, such as psychophysical tuning curves (PTCs). Normal-hearing (NH) listeners show sharp PTCs that are level- and frequency-dependent, whereas frequency selectivity is strongly reduced in cochlear implant (CI) users. This study aims at (a) assessing individual shapes of PTCs in CI users, (b) comparing these shapes to those of simulated CI listeners (NH listeners hearing through a CI simulation), and (c) increasing the sharpness of PTCs using a biologically inspired dynamic compression algorithm, BioAid, which has been shown to sharpen the PTC shape in hearing-impaired listeners. A three-alternative-forced-choice forward-masking technique was used to assess PTCs in 8 CI users (with their own speech processor) and 11 NH listeners (with and without listening through a vocoder to simulate electric hearing). CI users showed flat PTCs with large interindividual variability in shape, whereas simulated CI listeners had PTCs of the same average flatness, but more homogeneous shapes across listeners. The algorithm BioAid was used to process the stimuli before entering the CI users' speech processor or the vocoder simulation. This algorithm was able to partially restore frequency selectivity in both groups, particularly in seven out of eight CI users, meaning significantly sharper PTCs than in the unprocessed condition. The results indicate that algorithms can improve the large-scale sharpness of frequency selectivity in some CI users. This finding may be useful for the design of sound coding strategies particularly for situations in which high frequency selectivity is desired, such as for music perception.

Introduction

Frequency selectivity is an important characteristic determining the spectral resolution of the listener, which allows for the differentiation of spectral details in music and complex acoustic signals in everyday life. There are different psychoacoustic measures to assess the spectral resolution. For instance, auditory filter shapes can be determined using a notched-noise masking experiment (Patterson, Nimmo-Smith, Weber, & Milroy, 1982; Weber, 1977), or spectral resolution can be determined using spectral modulation thresholds (Litvak, Spahr, Saoji, & Fridman, 2007), which measure the smallest detectable spectral contrast in a stimulus with spectral ripples. A widely used technique to estimate frequency selectivity in normal-hearing (NH) or hearing-impaired (HI) listeners, however, is the use of psychophysical tuning curves (PTCs). Pure-tone PTCs display the masked threshold—that is, the level of a pure-tone masker that is necessary to render a specific target tone

[1]Medizinische Physik, Cluster of Excellence "Hearing4all," Carl von Ossietzky University, Oldenburg, Germany
[2]Forschungszentrum Neurosensorik, Carl von Ossietzky University, Oldenburg, Germany
[3]Department of Otolaryngology, Medical University Hannover, Hannover, Germany

Corresponding author:
Florian Langner, Department of Otolaryngology, Medical University Hannover, 30625 Hannover, Germany.
Email: langner.florian@mh-hannover.de

inaudible—as a function of different masker frequencies. A PTC can be measured with simultaneous masking or forward-masking paradigms (see Moore, Glasberg, & Roberts, 1984), each of which has its advantages and disadvantages and results in slightly different PTC shapes. Forward masking minimizes the possibility that lateral suppression of the probe by the masker may produce a masking effect (Moore, 1978), whereas simultaneous masking may produce a stimulus that is closer to ecologically relevant stimuli, such as speech in noise. Forward masking has been widely used in the psychoacoustic literature to estimate the auditory system's nonlinearity in the growth of masking experiments (e.g., Oxenham & Plack, 1997), for temporal masking curves (Nelson, Schroder, & Wojtczak, 2001), and frequency selectivity estimates, because it avoids problems associated with suppression. Therefore, a forward-masking paradigm was also chosen for the present study to estimate frequency selectivity.

In general, NH listeners show sharp PTCs with slightly lower masker level at threshold in the low-frequency tail (cf. Moore, 1978), due to upward spread of masking (cf. Nelson, 1991). PTCs are level-dependent with broader tuning at higher stimulus levels (Nelson, 1991). HI listeners show broader (shallower) PTCs than NH listeners (Florentine, Buus, Scharf, & Zwicker, 1980). This has been attributed in some HI listeners to the loss of outer hair cell function (Nelson, 1991). A recent study of Jürgens, Clark, Lecluyse, and Meddis (2016) showed that the broad PTC shape of HI listeners can be considerably sharpened when the psychoacoustic stimuli are preprocessed by the dynamic compression algorithm BioAid (Meddis, Clark, Lecluyse, & Jürgens, 2013), reintroducing two biological principles of the intact auditory system attributed to outer hair cells, that is, dynamic compression and frequency-selective feedback. This indicates that preprocessing algorithms based on biological principles can affect the PTC shape and thus may improve apparent frequency selectivity, for better distinction between signals of different frequency content, and thus potentially better acoustic object separation under certain circumstances.

In cochlear implant (CI) users, *spatial tuning curves* (Nelson, Donaldson, & Kreft, 2008; Nelson, Kreft, Anderson, & Donaldson, 2011) can be used to assess the spatial selectivity of electric stimulation on single electrodes using a similar forward-masking paradigm as used for measuring PTCs in NH and HI listeners. These spatial tuning curves are not normally measured using the CI user's personal speech processor, but with a research interface, which allows controlled stimulation of single or multiple electrodes. Spatial tuning curve shapes were found to be almost symmetric and highly individual across CI users, as well as across different stimulating electrodes (Nelson et al., 2011).

A direct comparison of spatial tuning curves in CI listeners to PTCs in NH and HI listeners is difficult, because such a comparison would require exact mappings of electric current to acoustic level and mappings of electrode location to acoustic (best) frequency. Furthermore, spatial tuning curves (measured using a research interface) do not necessarily reflect the frequency selectivity of the CI users in their everyday life, because their speech processor and sound coding strategy are not used during the course of the measurement. Simulated CI listeners, that is, NH listeners listening through a vocoder to simulate CI processing (Shannon, Zeng, Kamath, Wygonski, & Ekelid, 1995; Whitmal, Poissant, Freyman, & Helfer, 2007), could be used for facilitating such a comparison, bridging the gap between frequency selectivity measurements in CI and NH listeners.

The aim of this study was twofold: The first goal was to compare PTCs between simulated and actual CI users. Therefore, Experiment 1 of this study measured PTCs in simulated CI users with a vocoder, which contains realistic signal processing used in current sound coding strategies and mimics physiological details of actual CI users. In Experiment 2, the same psychoacoustic measurements were then performed with individual CI users, which means that PTCs were measured with the same acoustic stimuli (without vocoder processing), presented via the CI user's own speech processor. This approach allowed a direct comparison across individual CI users independent of CI manufacturer and device and also allowed for comparisons with NH listeners and simulated CI users. The second goal of this study was to test whether sharpening of the PTC shape due to preprocessing with the dynamic compression algorithm BioAid (Meddis et al., 2013) was possible in both simulated and actual CI users. The effects of two algorithm settings on PTC shape were investigated; these involved mimicking (a) healthy basilar membrane (BM) compression and (b) the function of the medial olivocochlear complex (MOC), both of which are assumed to be absent in CI listeners due to absence of outer hair cells. The hypothesis is that implementing these two biological principles in a preprocessing algorithm can help to improve the CI user's relatively poor frequency resolution (Friesen, Shannon, Baskent, & Wang, 2001).

Methods

Subjects

Eleven NH listeners (age range 22–30 years, average age of 26 years) acted as the simulated CI listeners listening through a software-implemented vocoder (adapted from Bräcker, Hohmann, Kollmeier, & Schulte, 2009, see below). The NH listeners had pure-tone thresholds

Table 1. Demographic information about all participating CI listeners.

ID	Age	Sex	Etiology	Duration of deafness (years)	CI usage (years)	Device
CI1	25	M	Ototoxic	17	8	Freedom Hybrid
CI2	23	F	Sudden hearing loss	0.5	3	CP810
CI3	45	M	Lack of oxygen	44	0.6	CP910
CI4	19	F	Unknown	8	12	OPUS 2
CI5	64	M	Meningitis	49	1	CP810
CI6	46	F	Sudden hearing loss	6	0.5	CP910
CI7	53	M	Progressive hearing loss	7	6	CP910
CI8	63	M	Sudden hearing loss	10	4	CP810

of less than 20 dB HL measured using standard audiometry (sinusoids with frequencies between 125 Hz and 8 kHz).

Eight actual CI listeners (postlingually deafened, see Table 1, average age of 42 years) participated in the study. These CI users were presented with acoustic sounds generated on a standard computer using an audio cable connected directly from the sound card to the input of their sound processor. Participants were offered regular breaks and were free to pause at any time during the experiment. All participants gave written consent prior to the experiment and were paid monetary compensation. Ethical consent was granted by the University of Oldenburg Ethical Committee.

Seven of the eight participants use CI devices by the manufacturer Cochlear Ltd., whereas one participant uses a MED-EL system. All Cochlear CI users used the Advanced Combinational Encoder (ACE) strategy, an NofM strategy stimulating only those N of the $M = 22$ electrodes with the highest amplitude within a stimulation frame. CI4 used MED-EL's Fine Structure Processing, which aims to implement the temporal fine structure of a signal by delivering bursts of stimulus pulses on the electrodes delivering low frequencies. These bursts are determined by the band-limited acoustic signal and cover a range of up to 950 Hz (Wouters et al., 2015).

Apparatus and Calibration

All listeners were seated in a sound-attenuating booth. The stimuli were generated on a standard PC with MATLAB (The MathWorks, Inc.) using customized scripts and were converted from digital to analog using an RME Fireface UC soundcard. The NH listeners were presented with stimuli via Sennheiser HDA 200 circumaural headphones. Stimulus levels were calibrated to dB SPL using a Bruel & Kjaer (B&K) 4153 artificial ear with a B&K ½ in. microphone type 4231, which was attached to a B&K 2610 measurement amplifier. CI listeners received the stimuli via the auxiliary input of their own CI speech processor and were asked to

choose the CI program that they mostly used in everyday life (if a program choice was possible).

The first stimulus presented via the auxiliary input (for the target threshold measurements) was set to −35 dB FS. Subsequent psychoacoustic testing was performed in relation to the measured absolute threshold of the target (i.e., in dB sensation level, SL). Absolute levels for the auxiliary input (e.g., in dB FS) were meaningless, because each device and each participant produced different digital levels (in dB FS) for the absolute target threshold.

Procedure

A three-interval-forced-choice (Levitt, 1971) one-up-two-down forward-masking paradigm was used to determine the individual masked thresholds for pure-tone maskers with seven frequencies relative (0.5, 0.7, 0.9, 1.0, 1.1, 1.3, and 1.7 times) to the fixed frequency of the 2-kHz pure-tone target. The target level was fixed at 10 dB SL, which was determined for each listener with an absolute threshold measurement of the pure-tone target beforehand using the same three-interval-forced-choice method. The 106-ms masker was followed by 10 ms of silence and the 16-ms target tone. Both stimuli were gated with 4-ms raised-cosine ramps. The masker was adaptively changed in level starting at a level of 10 dB SL and 10 dB level steps, reduced to 5 dB after the third reversal and to 1 dB after the sixth reversal. A measurement run was finished after the tenth reversal and the masked threshold of this run was defined as the average masker level at the last six reversals. Three measurement repetitions were averaged to obtain one masked threshold. All participants finished one measurement run (on-frequency) for familiarization with the measurement procedure. A training period was not implemented.

CI Simulation

A vocoder mimicking details of the signal processing and the physiology of CI users (Bräcker et al., 2009, Williges et
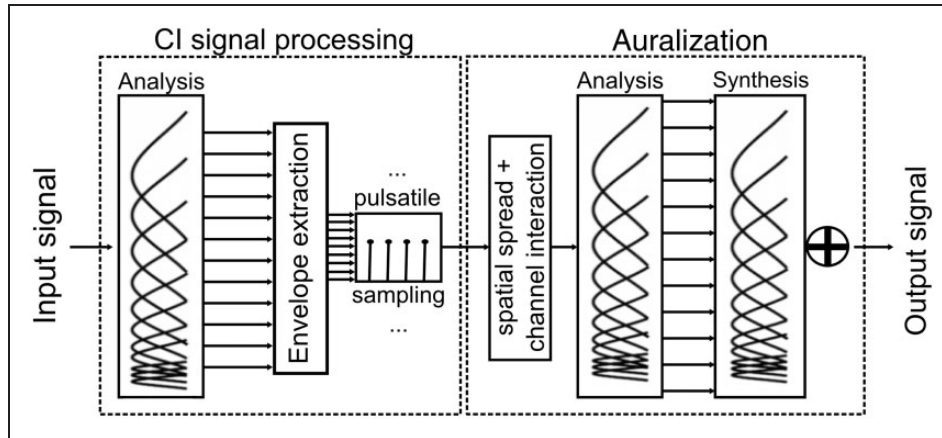
Figure 1. Block diagram of the CI simulation/vocoder. CI¼cochlear implant.

al. 2015) was used for simulating CI users with NH listeners. This vocoder was structured to resemble an implant type of brand Cochlear Ltd. with a Contour Advance electrode array consisting of 22 electrodes. The signal processing flow of this vocoder is shown in Figure 1.

The input signal (sampled at a rate of 22 kHz) is decomposed into 22 frequency channels using a third-order gammatone filterbank (Hohmann, 2002). The center frequencies of this analysis filterbank ranged from 250 Hz to 7438 Hz (see CI simulation column of Table 2) each with one equivalent rectangular bandwidth. These frequencies were chosen in agreement with the center frequencies of the Fast Fourier Transform bins used within Cochlear's ACE sound coding strategy (cf. Nogueira, Büchner, Lenarz, & Edler, 2005). The Hilbert envelope of the output of each channel was sampled at an average pulse rate of 1,000 pulses per second (i.e., 1/22 of the audio signal's sampling frequency), which is similar to the stimulation rate used in Cochlear devices. An 8-of-22 processing was implemented stimulating only the eight channels with highest amplitudes within a stimulation time frame (frame length 1 ms). The timing of this pulsatile sampling across electrodes was randomized within one frame, such that the signal in each channel is an envelope-weighted pulse train with a stochastic sequence of pulses. For simplicity, no amplitude compression was used in the vocoder to compress the envelopes in the frequency channels, in contrast to mappings of audio signal amplitude on current amplitude used within ACE (cf. Nogueira et al., 2005). Each pulse is multiplied by a two-sided exponentially decaying function a across the channels according to Equation (1) to simulate the spatial spread of the electric field in the perilymph. The decaying factor (denominator of the exponent in Equation (1)) was chosen to be 9 mm with nominator

Table 2. Center Frequencies of the Analysis Filterbank in the CI simulation and auralization part of the vocoder.

Channel number	CI simulation (Hz)	Auralization (Hz)
1	250	664
2	375	775
3	500	902
4	625	1046
5	750	1210
6	875	1396
7	1000	1608
8	1125	1849
9	1250	2123
10	1438	2435
11	1688	2789
12	1938	3192
13	2188	3651
14	2500	4173
15	2875	4766
16	3313	5441
17	3813	6208
18	4375	7081
19	5000	8074
20	5688	9204
21	6500	10488
22	7438	11950

$|d|$ as the absolute distance in mm from the stimulating electrode.

$$\alpha = e^{\left(-\frac{|d|}{9\,\mathrm{mm}}\right)} \tag{1}$$

In the auralization part, each channel is filtered again with a third-order gammatone filterbank but with different center frequencies (664 to 11950 Hz, see auralization column of Table 2) in order to simulate the mapping of each frequency channel to electrode location. The center frequencies of this second analysis filterbank were chosen to be the best frequencies corresponding to the electrode positions of the Cochlear Contour Advance electrode array with an insertion depth of 24 mm in a 32 mm human cochlea, calculated using Greenwood's (1990) place-frequency map. A synthesis filterbank with the same center frequencies as this second analysis filterbank compensates for filter group delays (Hohmann, 2002) and produces the (mono) signal to be presented to the NH listeners.

In summary, the vocoder signal thus consists of narrow bandpass-filtered carriers (with a stochastic, noise-like fine structure), of envelopes corresponding to the sampled envelopes that are spectrally smeared due to the spatial spread function, and carriers that are shifted in frequency according to the chosen electrode-to-best-frequency mapping.

BioAid Processing

The signal processing flow of the multichannel dynamic compression algorithm BioAid (Meddis et al., 2013) is shown in Figure 2. BioAid mimics two essential
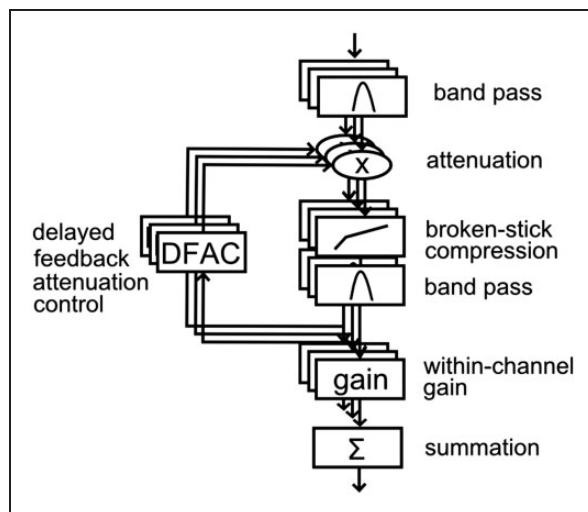
Figure 2. Signal processing structure in the BioAid algorithm; different layers symbolize different frequency channels. Reprinted with permission of Taylor & Francis Ltd, www.tandfonline.com on behalf of (copyright ©) British Society of Audiology; International Society of Audiology; Nordic Society of Audiology, from Jürgens et al. (2016), "Exploration of a physiologically-inspired hearing-aid algorithm using a computer model mimicking impaired hearing," *International Journal of Audiology*, 55(6), 346–357.

mechanisms in the healthy auditory system: The first mechanism is the instantaneous compression of the BM, which is technically realized by an instantaneous *broken-stick* compression. The second mechanism is the reflex of the MOC which is realized by a slow and time-delayed feedback loop. In detail, nine Butterworth band-pass filters were used, of which three were octave-wide (center frequencies of 250 Hz, 500 Hz, and 1 kHz) and six half-octave-wide (center frequencies between 1.4 kHz and 8 kHz) at half-octave spacing to decompose the signal into frequency channels. Within each frequency channel, the signal is processed using an instantaneous broken-stick compression with a fixed compression ratio of 5:1 and a parameterized compression threshold, followed by a second bandpass filter with the same characteristics as the first bandpass filter. Such a combination of instantaneous compression and bandpass filtering was also used for the nonlinear path of the dual resonance nonlinear filterbank of Lopez-Poveda and Meddis (2001) in order to realistically simulate BM compression.

The MOC reflex is simulated in the BioAid algorithm as a within-channel feedback loop, which adaptively attenuates the output of the first bandpass filter dependent on the average level present in the output of the second bandpass filter. This technical realization is called delayed feedback attenuation control (DFAC) and is inspired by and in agreement with physiological data about the time course and strength of the MOC reflex. The implementation is identical in each channel (i.e., not frequency-dependent). The time constant of the adaptive attenuation is set to 50 ms (cf. Backus & Guinan, 2006) and a 10 ms delay between output of the second bandpass filter and application of the attenuation is used to simulate neuronal delays in the MOC reflex loop. The (variable) parameter of this DFAC is the DFAC threshold, which indicates at which (input) level the attenuation starts to be applied. The attenuation values are calculated by first subtracting the DFAC threshold from the power envelope of the output of the second bandpass filter, temporally smoothing, and linear mapping these values on a scale between 0 dB and a maximum of 20 dB. The level-dependence of the DFAC feedback loop thus interacts with the compressive nonlinearity (if enabled).

Both physiological mechanisms (healthy BM compression and MOC reflex) are missing in CI listeners, which is why their imitation might improve or even restore frequency selectivity. The next processing step of BioAid is a within-channel gain (used also in Jürgens et al., 2016 to amplify the signal for HI listeners), which was deactivated in the current study. The summation of the signals in each channel forms the actual (mono) signal that is being presented or processed further. Note that this summation is not physiologic but

was done in this study to test the same algorithm as in Jürgens et al. (2016) with CI listeners for comparison aspects.

The parameters for both the instantaneous compression and the DFAC are individually set for each NH and CI listener. The hearing threshold of the 16 ms target tone was measured beforehand to obtain these values. The DFAC threshold is set to the same dB SPL value as the target tone during the PTC experiment (i.e., 10 dB SL), while the threshold for the instantaneous compression was set 5 dB above this value (therefore at 15 dB SL). These settings are in rough agreement with physiological observations (Russell & Murugasu, 1997) showing that the DFAC's physiological counterpart MOC is strongest close to absolute threshold, whereas the instantaneous compression is active at levels above threshold (Ruggero et al. 1997; Russell & Murugasu, 1997). The exact values in humans are not known and, for example, the compression threshold may be highly individual even across NH listeners (Plack, Drga, & Lopez-Poveda, 2004).

PTCs were measured for simulated and actual CI users in three conditions: unprocessed (i.e., vocoder-only for simulated CI listeners), BioAid without instantaneous compression, and BioAid with instantaneous compression. These two BioAid conditions were chosen to investigate the effect of either mimicking MOC processing alone or mimicking the combination of MOC processing and BM compression, as both have shown frequency selectivity improvements in HI listeners (Jürgens et al., 2016). In addition, NH listener's PTCs were measured without any processing (vocoder or BioAid) as a reference. The presentation order of the conditions was pseudorandomized for each listener. All measurements in one condition were completed before the next condition was started. All three repetitions as well as the order of masker frequencies in each condition were measured in an interleaved manner.

Results

Figures 3 and 4 show PTCs as masker threshold levels in dB SL, which means that the 0 dB SL line indicates the absolute threshold of the target tone. This display was chosen, because absolute sound pressure level specifications for CI listeners presented with stimuli via their auxiliary sound input were not possible and the dB SL allows for direct comparisons between simulated
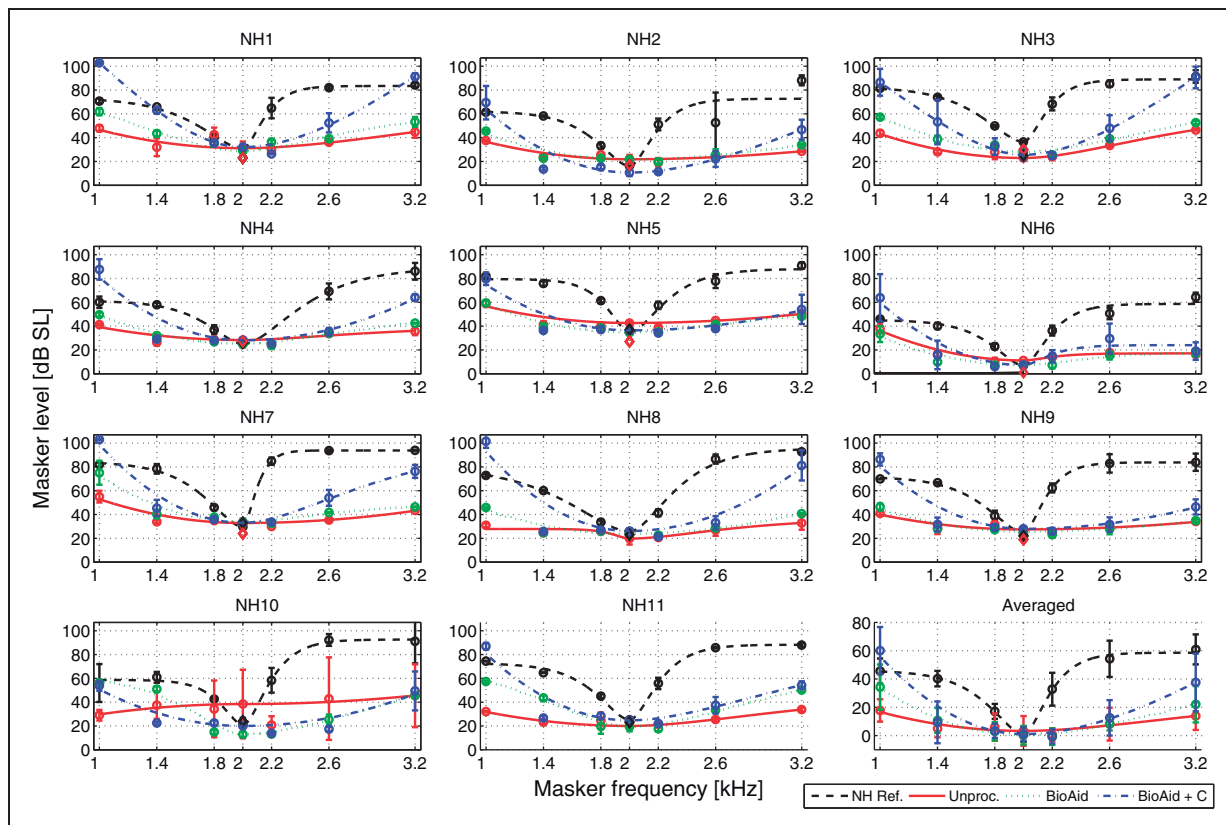
Figure 3. Individual PTCs of all 11 simulated CI listeners and PTCs averaged across all listeners. Bottom left panel: Masker level in dB SL as a function of masker frequency in kHz. Error bars indicate one standard deviation from the mean.
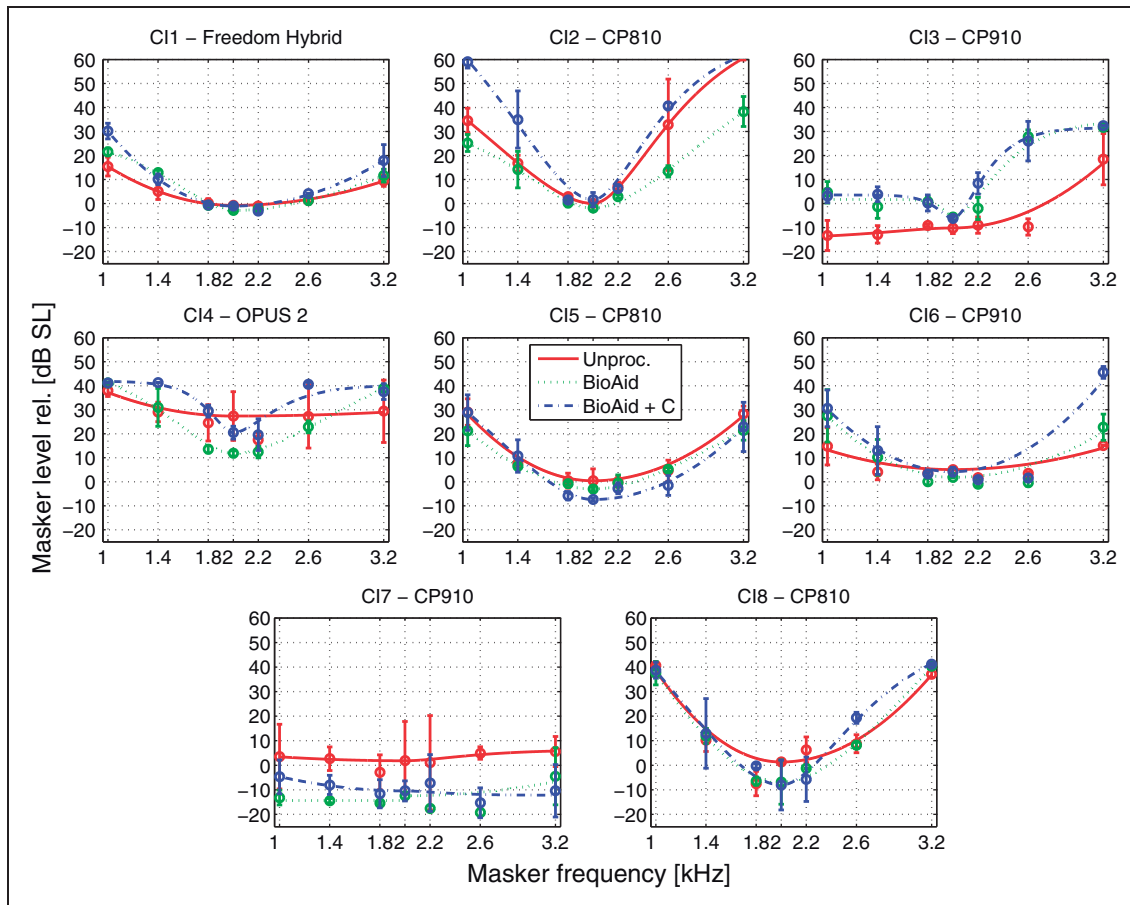
Figure 4. Individual PTCs of eight actual CI listeners measured with three preprocessing conditions: Relative masker level in dB SL as a function of masker frequency in kHz. Error bars indicate one standard deviation from the mean.

and actual CI listeners. Circles indicate the averages over all three measurement repetitions for a masker frequency, while error bars indicate one standard deviation over the three repetitions. PTCs were fitted using a second-order rounded exponential fit (Patterson et al., 1982).

Experiment 1—Simulated CI Listeners

Figure 3 shows individual PTCs (masked thresholds as a function of masker frequency) averaged over the three measurement runs. In addition, the PTC averaged across all participants is shown in the bottom right panel. For each individual listener, a similar pattern can be observed. The NH reference PTC (black dashed line) is relatively sharp with high masked thresholds (around 40 dB to 60 dB SL) at the outer frequencies (1, 1.4, 2.6, and 3.2 kHz). The unprocessed CI simulation (realized using the vocoder only, red continuous line) shows a flat shape in all listeners. BioAid without instantaneous compression (i.e., with DFAC only, green dotted line) shows small improvements in frequency selectivity in

terms of a sharper PTC curve and higher masked thresholds at the outermost masker frequencies (1 and 3.2 kHz). The improvement is stronger using BioAid with instantaneous compression (blue dashed-dotted line), which is also evident at the outermost frequencies, whose average masker levels are about 20 dB higher than in the PTC collected with BioAid without instantaneous compression. Relatively large error bars in the averaged results (bottom right panel) originate in interindividual differences and not in large error bars in individual PTCs.

Experiment 2—Actual CI Listeners

Individual PTCs for actual CI listeners showed larger variability in form among subjects (Figure 4) than for simulated CI listeners. In most cases, the unprocessed condition (red continuous lines) resulted in a relatively flat PTC shape (similar to the unprocessed PTC of simulated CI listeners, see Figure 3). High variability in PTC shape can also be observed regarding the effect of preprocessing the stimuli with BioAid. BioAid without
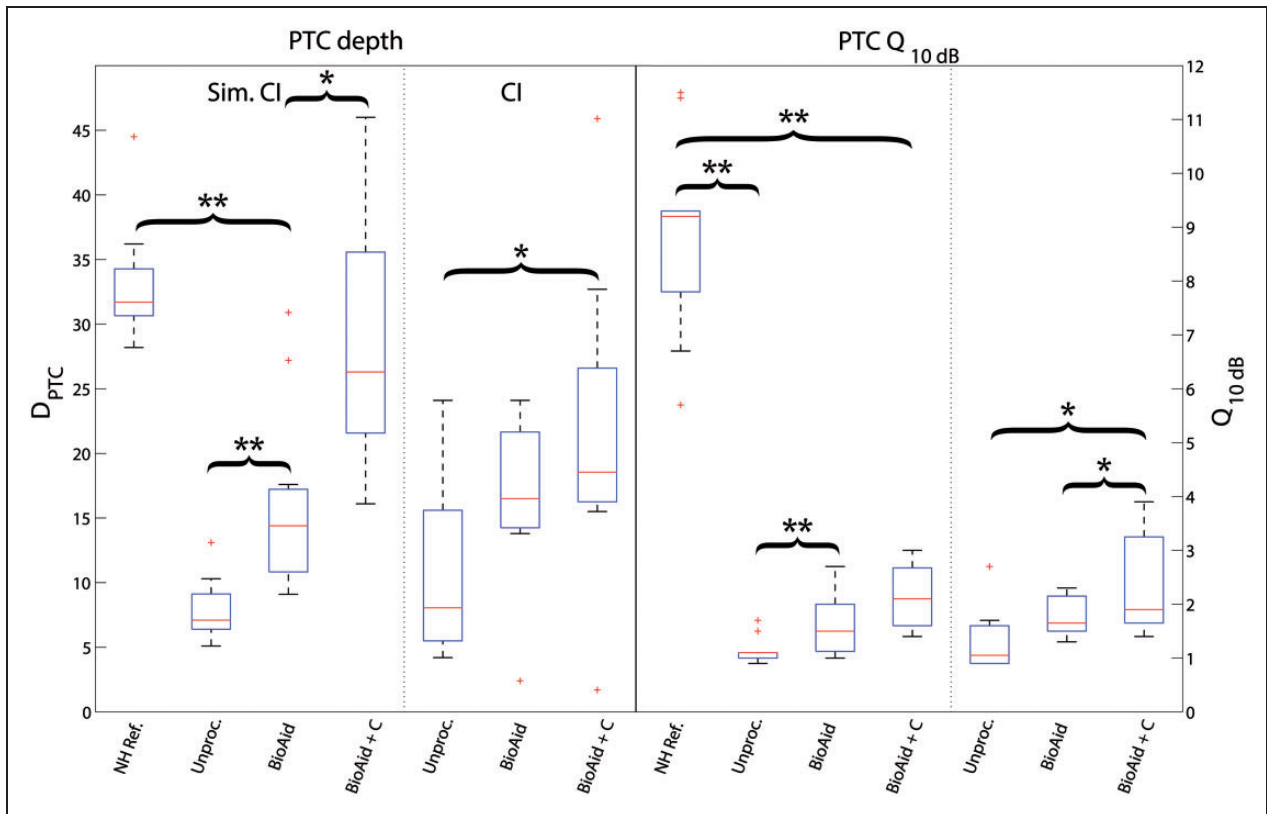
Figure 5. Boxplots showing D_{PTC} and PTC_{Q10dB} for simulated and actual CI listeners: The horizontal line within the box indicates the median; edges are the 25th and 75th percentiles, whiskers the most extreme data points, and outliers are shown as plus signs. Significance symbols indicate $p < .05$ with * and $p < .01$ with **. PTC = psychophysical tuning curve.

instantaneous compression resulted in slightly sharper PTCs for some CI listeners (CI2, 3, 4, 6, and 8), while PTCs in other CI listeners showed almost no change (CI1, 5, and 7). For BioAid with instantaneous compression (blue dashed-dotted line), the PTC shape was strongly (Q_{10dB} improvement over unprocessed condition greater than 1.5 like CI2, CI3, and CI4, see below), modestly (Q_{10dB} improvement over unprocessed condition between 0.5 and 1.5 like CI1, CI5, CI6, and CI8), or not at all (CI7) affected by the algorithm. Thus, BioAid had a much stronger frequency selectivity restoration effect with than without instantaneous compression, especially in terms of higher masked thresholds at the outer masked frequencies (1, 1.4, 2.6, and 3.2 kHz).

Statistical Comparisons

Statistical comparisons were conducted to quantify the sharpness of PTC shape with two different measures: D_{PTC} (cf. Lecluyse, Tan, McFerran, & Meddis, 2013) and Q_{10dB}. D_{PTC} is a depth measure, in dB, and is defined as the difference between the average masker levels at all four outlying masker frequencies and the average of the masker levels at the three center masker

frequencies. This measure is suitable for capturing the large-scale shape of the PTC. Thus, PTC sharpness can be classified as strong (above 20 dB), medium (10–20 dB), or low (below 10 dB). Q_{10dB} is the ratio between the center frequency and the bandwidth 10 dB above the tip of the curve. For relatively flat PTCs, Q_{10dB} captures variations more near the center frequencies and is therefore a small-scale measure for PTC shape comparisons. For both D_{PTC} and Q_{10dB}, high values indicate sharper PTCs. The Friedman test with Bonferroni correction applied was used for statistical comparisons.

Figure 5 shows boxplots of D_{PTC} (left side) and Q_{10dB} (right side) extracted from individual simulated and actual CI listeners. Curly brackets indicate significant (*) or highly significant (**) differences. For the simulated CI listeners, D_{PTCs} were significantly different between the unprocessed condition and both BioAid conditions ($p < .01$), as well as significantly different between both BioAid conditions ($p < .05$). No significant difference was found between BioAid with instantaneous compression and the NH reference ($p > .1$), suggesting that the PTC sharpness (as measured using the large-scale shape measure D_{PTC}) is similar to the NH reference. Significant differences in Q_{10dB} were found between the unprocessed and both BioAid conditions ($p < .01$).

However, the NH reference condition showed a highly significant difference in Q_{10dB} to all other conditions ($p < .01$) indicating that the small-scale shape of the PTC (as well as their visual form) is not restored.

The median D_{PTC} and Q_{10dB} of actual CI listeners match the respective median values of the simulated CI listeners in the unprocessed condition. However, the larger boxplots of actual CI listeners in the unprocessed condition confirm a larger variability across actual CI listeners compared with the simulated CI listeners (D_{PTC} range of 2.7 dB for simulated and 10.1 dB for actual CI listeners of the 25th and 75th percentiles). A significant difference between the unprocessed condition and BioAid with instantaneous compression was found for actual CI listeners both regarding D_{PTC} and Q_{10dB} ($p < .05$). There was no statistical difference in D_{PTC} or Q_{10dB} between unprocessed and BioAid without instantaneous compression in actual CI listeners. This indicates that frequency selectivity could be improved in actual CI listeners by using BioAid with instantaneous compression but not without.

Potential training effects across the three different measurement repetitions (runs) were investigated using a two-way repeated measures analysis of variance with factors masker frequency and measurement repetition. Table 3 shows significance values (p-values) for each measurement condition separately. The effects of masker frequency were highly significant across all measurement conditions, whereas no significant effect of measurement repetitions was found in any measurement condition, indicating the absence of a training effect across the three measurement runs. Additionally, an interaction effect between masker frequency and measurement repetition is absent as well.

Discussion

This study measured individual PTCs in simulated and actual CI listeners with and without preprocessing the psychoacoustic stimuli by the multichannel dynamic compression algorithm BioAid.

Comparison Between Simulated and Actual CI Listeners in Unprocessed Condition

Flat PTCs were found in simulated and actual CI listeners without BioAid processing in comparison to the relatively sharp NH reference PTC. The sharpness of the NH reference PTC is in line with the PTC sharpness found in other studies using a forward-masking paradigm (Moore et al., 1984; Nelson, 1991). In contrast, the average flatness of PTCs in simulated CI listeners matches the average flatness of PTCs in actual CI listeners in the current study quantified by both the D_{PTC} and Q_{10dB}. This highlights that frequency selectivity can be realistically simulated using the vocoder of the current study (Bräcker et al., 2009,Williges et al. 2015), which includes a function mimicking the spatial spread of the electrical field in the perilymph. The exponentially decaying shape of this spatial spread function *smears* information across frequency and thus reduces frequency selectivity. This approach may contribute to the limited amount of available separate spectral channels in actual CI users (Friesen et al., 2001). Similar approaches have been used to simulate the effects of spread of excitation on speech identification in stationary noise (Bingabr et al., 2008), modulated noise (Fu & Nogaki, 2005), and both tone and noise maskers (Oxenham & Kreft, 2014), as well as effects of channel interaction on melodic pitch perception (Crew, Galvin, & Fu, 2012). Furthermore, direct links between simulated spectral resolution in a vocoder, measured spectral modulation thresholds, and speech recognition were found (Litvak et al., 2007), highlighting the importance of spectral resolution in simulated and actual CI users for their perception of a variety of stimuli.

Concerning the PTC form, the NH reference PTC shows lower masker thresholds within the low-frequency tail compared with the high-frequency tail (at the same distance to the target's frequency) in agreement with, for example, Nelson et al. (1991). In contrast, flat PTCs in simulated CI listeners show slightly higher masker thresholds within the PTC's low-frequency tail, again

Table 3. Significance Values (p) of the Within-Subject Effects of Masker Frequency, Measurement Repetition, and Their Interaction for All Measurement Conditions and Both Subjects Groups.

Factor	Simulated CI listeners				CI listeners		
	Normal-hearing reference	Unprocessed	BioAid	BioAid + C	Unprocessed	BioAid	BioAid + C
Masker Frequency	< 0.001	<0.001	<0.001	<0.001	<0.001	<0.001	<0.001
Repetition	.098	.391	.793	.054	.099	.097	.124
Interaction Masker Frequency × Repetition	.257	.546	.670	.184	.090	.893	.100

due to the spatial spread function used within the CI simulation. The spatial spread function is symmetric along the cochlear partition, that is, symmetric on a logarithmic frequency scale, which explains its slight asymmetry on the linear frequency scale in the average data of Figure 3. PTCs in actual CI listeners without BioAid processing show flat but nonsystematic shapes across individuals.

Sources of Individual Differences in CI Listeners

The similarity of PTC shapes across simulated CI listeners contrasts with the very individual PTC shapes across the actual CI listeners. This large variability (see Figure 4) is in line with variability in CI listener's spatial tuning curves reported in Nelson et al. (2008, 2011). Anderson, Nelson, Kreft, Nelson, and Oxenham (2011) showed that this variability in spatial tuning curves correlates also with another measure of spectral resolution in CI users, namely spectral ripple discrimination. Different physiological factors may have contributed to this high degree of variability. These factors could be the individual spatial spread of the electric field in the perilymph, which may occur due to different distances between electrode and auditory nerve tissue in individuals, number and distribution of auditory nerve fibers (Fayad & Linthicum, 2006; Zhu, Tang, Zeng, Guan, & Ye, 2012), differences in electrode-nerve interface (Bierer & Nye, 2014), and the individual and electrode-dependent electric dynamic range (Chatterjee, Fu, & Shannon, 2000). However, also two different signal processing schemes (as well as four different devices and implant types from two different manufacturers) may have contributed to this variability as well. These factors can, in principle, be implemented also in the vocoder being used in this study (Bräcker et al., 2009, Williges et al. 2015) for a systematic investigation of how strong the influence of these factors is on the PTC shape.

PTC sharpening was also observed in two different forms, one which lowered the tip but left the sides almost unchanged (as in CI8) and the more common case, which left the tip unchanged and increased the sides (as in CI2). The former case may be interpreted as that CI8 benefits more from the temporal mechanism of the DFAC, reducing the masker's amplitude in the on-frequency condition, but not so much from the frequency-selective mechanism, which mostly affects the remote off-frequency maskers (details see below). A possible (hypothetical) reason could be a greater spread of the electric field in this listener, which limits spectral resolution and which may limit possible benefits in tolerating off-frequency maskers.

Effect of BioAid Algorithm on PTCs

In line with earlier findings in HI listeners (Jürgens et al., 2016), the PTC shape was sharpened in all simulated CI listeners and in seven out of eight actual CI listeners due to the algorithm BioAid. This indicates that frequency selectivity as measured in the current study can be improved for all those CI devices tested in this study by an algorithm processing the stimuli before entering the CI sound coding strategy. The introduction of the D_{PTC} measure revealed that predominantly the large-scale shape of the PTC was affected, that is, masked threshold increases were mainly present at remote masker frequencies. Frequency selectivity changes at nearby masker frequencies were limited, as the Q_{10dB} measure showed. Listener CI7 showed the shallowest unprocessed PTCs, which indicated that for this listener, even remote off-frequency maskers were as effective in masking the target as on-frequency maskers. Interestingly, this listener also showed relatively poor speech intelligibility. PTCs stay flat also with preprocessing using BioAid. The reason for the lack of frequency selectivity improvement in this listener (CI7) is currently not clear. It is, however, likely that the unprocessed off-frequency masker levels are so low that they are situated at or below the DFAC threshold and that the BioAid processing thus has virtually no effect on the masker as well as on the target. This indicates that a slight increase in masker level with distance from the target frequency in the unprocessed condition is necessary in order to see the improvement effect.

Mechanisms Responsible for the Effect on PTCs

Two different mechanisms in BioAid are responsible for the improvements in frequency selectivity (as measured using PTCs), which can be separated by the two BioAid processing conditions tested in this study. The effect of BioAid's DFAC is outlined in Figure 6, which shows typical composite output signals of BioAid (i.e., added across bands) to the masker and probe sequence used for measuring the on-frequency masker threshold of a PTC (Figure 6(a)), and for measuring the off-frequency masker threshold (Figure 6(b), with masker frequency one octave below the target frequency). Note that the *input level* of the target tone is the same across Figure 6(a) and (b), although the target's output amplitude differs visibly. In the on-frequency case, both the masker and target tone are processed in the same frequency channel. The within-channel DFAC feedback loop attenuates the masker increasingly during its time course and also attenuates the target tone, because the target tone follows after a 10 ms gap, which is too short to reduce the DFAC's attenuative function. Thus, masker and target are equally affected due to the DFAC and masker thresholds are virtually unchanged in comparison to the unprocessed condition. In the off-frequency case (Figure 6(b), i.e., for remote masker frequencies), however, masker and target tone are
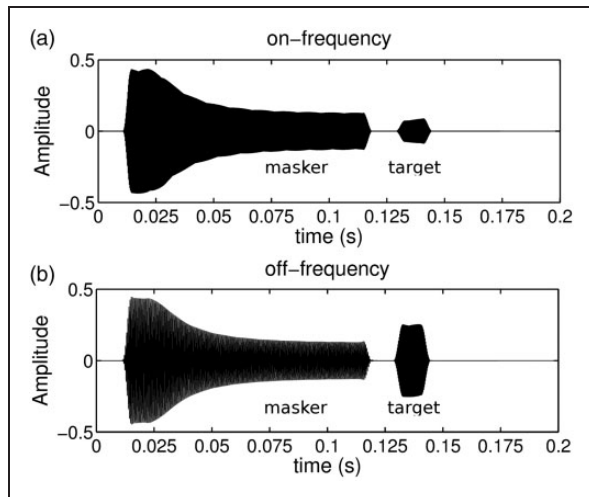
Figure 6. Principle of the DFAC process for the on-frequency (a) and off-frequency case (b): Application of attenuation on the masker after exceeding the DFAC threshold and effect on the target tone when processed in the same (a) or different (b) frequency band.

processed in *different* frequency channels. The attenuation of the masker is the same as in Figure 6(a), because the DFAC loop implemented in the masker's channel is affecting the masker's amplitude. However, there is virtually no attenuation of the target's amplitude, because the DFAC attenuation works within-channel only. The signal in the on-frequency channel is thus hardly affected from the masker. Therefore, the masking effect for maskers with remote frequencies is diminished, allowing higher masker levels at threshold for the PTC. Thus, the specific channel arrangement in BioAid and the within-channel DFAC processing allows higher masker thresholds at 1, 1.4, 2.6, and 3.2 kHz in comparison to virtually unchanged masker thresholds at 1.8, 2, and 2.2 kHz. This processing is in line with physiological studies showing that the efferent feedback loop attenuates ongoing signals near the center frequency of the stimulus, but that the same attenuation caused by the stimulus is not applied to other (more remote) frequencies (Cooper & Guinan, 2006).

A further parallel can be made to studies investigating tuning curves with or without stimulating the MOC permanently. Cooper and Guinan (2006) and Jennings and Strickland 2012 showed that permanently eliciting the MOC electrically or by using a precursor stimulus reduces frequency resolution. By permanently eliciting the MOC, the actual functionality of the MOC for the test stimuli is diminished in their studies. However, the introduction of BioAid in the present study has a different effect than eliciting the MOC permanently. By introducing BioAid, the functionality of time-dependent attenuation to the composite system is re-obtained,

which sharpens frequency selectivity by means of the mechanism outlined earlier.

Enabling instantaneous compression in addition to the DFAC (in BioAid + instantaneous compression) has an additional restorative effect on frequency selectivity. The compression threshold is set such that the target tone (at 10 dB SL) is always uncompressed, whereas the masker can be compressed, especially if higher masker levels are present such as at remote masker frequencies. This diminishes the masking effect for remote-frequency maskers further, allowing even higher masker levels for these frequencies and sharpening the resulting PTC. Note that in contrast to the mechanism of DFAC without compression, this mechanism may not be in line with physiology, because off-frequency signals are most likely not processed compressively in the on-frequency channel (Ruggero et al., 1997). Thus, enabling compression should not affect the masker's ability to mask the target in the on-frequency channel additionally.

Differences Between Simulated and Actual CI Listeners

Frequency selectivity improvements were on average smaller in actual than in simulated CI listeners. Likely reasons for these differences are the different compression stages active in these two groups of listeners. While simulated CI listeners use only one compression stage in BioAid with instantaneous compression (in addition to their healthy BM compression), actual CI listeners use up to three compression stages, which are (a) BioAid with instantaneous compression, (b) a broadband automatic gain control or adaptive dynamic range optimization (Blamey, 2005) preceding, and (c) instantaneous compression within their sound coding strategy. Thus, also PTCs in an *unprocessed* condition may be more compressed in actual than in simulated CI listeners, leaving less room for frequency selectivity improvements.

Perspectives of Improving Frequency Selectivity for Speech Enhancement

This study showed improvements in frequency selectivity for CI users with relatively artificial, controlled stimuli. The mechanism of BioAid outlined above is likely to be most effective if desired signal and undesired signal (such as noise) have distinct spectral content, because of the frequency-selective processing of the DFAC. Furthermore, the findings here were obtained in a forward-masking paradigm and their transfer to simultaneous masking techniques remains to be tested. Spectral modulation thresholds (Litvak et al., 2007) for instance may on the one hand be improved by the algorithm if the spacing between different independently acting frequency

bands of BioAid is dense enough to allow frequency-specific processing for the spectral ripple stimuli. On the other hand, there may also be a detrimental effect on spectral modulation thresholds due to the compression introduced with BioAid (similar as the effect in multichannel hearing aids, Plomp, 1988). Frequency selectivity using notched-noise paradigms (e.g., Patterson et al., 1982) may be improved by the BioAid algorithm, particularly if a forward-masking paradigm is used. Thus, future studies should investigate if the improvements in frequency selectivity in HI (Jürgens et al., 2016) and CI listeners (current study) will persist also with other techniques, particularly in simultaneous masking paradigms, to measure frequency selectivity.

Improvements in frequency resolution for more complex stimuli remain also to be tested both in CI and HI listeners. Speech and babble noise, for example, have similar spectral content, which could mean that their separation may not be particularly improved by the outlined mechanism. However, an improvement of speech and noise separation (especially at positive signal-to-noise ratios) is still possible, because the auditory model used as a blueprint for the DFAC has shown better speech discriminability with than without efferent processing enabled (Clark et al., 2012). It is, nevertheless, important to note that other studies that aimed at improving the spectral contrast for CI users have shown only limited (Bhattacharya & Zeng, 2007; Nogueira, Rode, & Büchner, 2016; Oxenham, Simonson, Turicchia, & Sarpeshkar, 2007) improvements for speech in noise performance for CI listeners. It should thus also be tested if the improvements in frequency selectivity by BioAid also go along with better speech intelligibility in noise for CI users.

Perspectives for BioAid's Principles in a Sound Coding Strategy

We were able to acquire participants using devices from two of the main CI manufacturers: Cochlear and MED-EL. Both manufacturers use a different sound coding strategy, resulting in potentially different effects of BioAid's processing. We suspect that effects of the sound coding strategies on the PTC measurement with and without BioAid are small, since only pure tones were used in the experiments, which were presented subsequently. For the types of narrow-band stimuli used here, both ACE (picking spectral peaks and disregarding spectral valleys) and CIS (stimulating in a round-robin manner) should produce very similar outputs, however, potentially differing in their stimulation rate.

It is conceivable that the direct implementation of BioAid's mechanisms into a CI sound coding strategy will avoid the *unphysiologic* summing of the signal across bands, because the signal within a frequency band can be transmitted directly to one electrode. This may enlarge BioAid's frequency selectivity restoration effect, because the compressive processing within the strategy can be synchronized with the compressive and feedback characteristics of BioAid. This might be useful for alleviating the distinction of frequencies in tone complexes, which may improve CI listener's relatively poor pitch perception (Geurts & Wouters, 2001), leading in turn also to improved music perception (cf. Laneau, Wouters, & Moonen, 2006). However, it is important to also consider the simultaneous effects on speech perception. While improved frequency selectivity, and thus access to more spectral channels, in principle should be advantageous for speech-in-noise performance in CI listeners (Friesen et al., 2001), compressive processing itself might be disadvantageous for speech recognition (cf. Jürgens, Ewert, Kollmeier, & Brand, 2014) by reducing the contrast between peaks and troughs in the speech's modulation. Thus, further studies are needed in order to explore the optimal settings of this compressive processing and their effect on frequency selectivity and speech intelligibility within a CI sound coding strategy.

Conclusions

This study assessed and compared PTCs of simulated and actual CI users. Furthermore, the dynamic compression algorithm BioAid was used to preprocess acoustic stimuli before entering the vocoder used for the CI simulation or the CI user's own speech processor. The following conclusions can be drawn.

1. Unprocessed PTCs of simulated CI users were found to be broader than the NH reference PTC. Unprocessed PTCs of actual CI users were found on average as broad as in simulated CI users, but the variation of PTC shape across actual CI users was much higher.
2. In both groups, the algorithm BioAid was able to partially restore the sharpness of PTCs, except for one CI user (CI7). Particularly the large-scale shape of the PTCs was affected, that is, remote masker thresholds were much higher than unprocessed. This indicates that frequency selectivity (as measured using PTCs in a forward-masking paradigm) can be improved using a compressive processing preceding the CI speech processor.

Future research should investigate the implementation of BioAid's algorithm structure directly into a sound coding strategy for CIs (rather than preprocessing the acoustic stimuli). It will be important to find out whether the improvement in PTC shape has other benefits, even in other measures of frequency selectivity. Thus, it remains an open question whether this approach

could help in speech perception, although the results from earlier work showed limited improvements.

References

Anderson, E. S., Nelson, D. A., Kreft, H., Nelson, P. B., & Oxenham, A. J. (2011). Comparing spatial tuning curves, spectral ripple resolution, and speech perception in cochlear implant users. *The Journal of the Acoustical Society of America*, 130(1), 364–375.

Backus, B. C., & Guinan, J. (2006). Time-course of the human medial olivocochlear reflex. *Journal of the Acoustical Society of America*, 119(5), 2889–2904.

Bierer, J. A., & Nye, A. D. (2014). Comparisons between detection threshold and loudness perception for individual cochlear implant channels. *Ear & Hearing*, 35(6), 641–651.

Bingabr, M., Espinoza-Varas, B., & Loizou, P. C. (2008). Simulating the effect of spread of excitation in cochlear implants. *Hearing Research*, 241(1–2), 73–79.

Bhattacharya, A., & Zeng, F. G. (2007). Companding to improve cochlear-implant speech recognition in speech-shaped noise. *The Journal of the Acoustical Society of America*, 122(2), 1079–1089.

Blamey, P. J. (2005). Adaptive dynamic range optimization (ADRO): A digital amplification strategy for hearing aids and cochlear implants. *Trends in Amplification*, 9(2), 77–98.

Bräcker, T., Hohmann, V., Kollmeier, B., & Schulte, M. (2009). Simulation und Vergleich von Sprachkodierungsstrategien in Cochlea-Implantaten [Simulation and comparison of speech coding strategies in cochlear implants]. *Zeitschrift der Audiologie /Audiological Acoustics*, 48(4), 158–169.

Chatterjee, M., Fu, Q. J., & Shannon, R. V. (2000). Effects of phase duration and electrode separation on loudness growth in cochlear implant listeners. *Journal of the Acoustical Society of America*, 107(3), 1637–1644.

Clark, N. R., Brown, G. J., Jürgens, T., & Meddis, R. (2012). A frequency-selective feedback model of auditory efferent suppression and its implications for the recognition of speech in noise. *Journal of the Acoustical Society of America*, 132, 1535–1541.

Cooper, N. P., & Guinan, J. J. Jr (2006). Efferent-mediated control of basilar membrane motion. *The Journal of Physiology*, 576, 49–54.

Crew, J. D., Galvin, J. J. III, & Fu, Q.-J. (2012). Channel interaction limits melodic pitch perception in simulated cochlear implants. *Journal of the Acoustical Society of America*, 132(5), 429–435.

Fayad, J. N., & Linthicum, F. H. Jr (2006). Multichannel cochlear implants: Relation of histopathology to performance. *The Laryngoscope*, 116(8), 1310–1320.

Florentine, M., Buus, S., Scharf, B., & Zwicker, E. (1980). Frequency selectivity in normally-hearing and hearing-impaired observers. *Journal of Speech Language and Hearing Research*, 23(3), 646–669.

Friesen, L. M., Shannon, R. V., Baskent, D., & Wang, X. (2001). Speech recognition in noise as a function of the number of spectral channels: Comparison of acoustic hearing and cochlear implants. *Journal of the Acoustical Society of America*, 110(2), 1150–1163.

Fu, Q. J., & Nogaki, G. (2005). Noise susceptibility of cochlear implant users: The role of spectral resolution and smearing. *Journal of the Association for Research in Otolaryngology*, 6, 19–27.

Geurts, L., & Wouters, J. (2001). Coding of the fundamental frequency in continuous interleaved sampling processors for cochlear implants. *Journal of the Acoustical Society of America*, 109(2), 713–726.

Greenwood, D. (1990). A cochlear frequency-position function for several species - 29 years later. *Journal of the Acoustical Society of America*, 87(6), 2592–2605.

Hohmann, V. (2002). Frequency analysis and synthesis using a Gammatone filterbank. *Acta Acoustica*, 88(3), 433–442.

Jennings, S. G. & Strickland, E. A. (2012). Evaluating the effects of olivocochlear feedback on psychophysical measures of frequency selectivity. *Journal of the Acoustical Society of America*, 132(4), 2483–2496.

Jennings, S. G., Heinz, M. G., & Strickland, E. A. (2011). Evaluating adaptation and olivocochlear efferent feedback as potential explanations of psychophysical overshoot. *Journal of the Association for Research in Otolaryngology*, 12(3), 345–360.

Jürgens, T., Clark, N. R., Lecluyse, W., & Meddis, R. (2016). Exploration of a physiologically-inspired hearing-aid algorithm using a computer model mimicking impaired hearing. *International Journal of Audiology*, 55(6), 346–357.

Jürgens, T., Ewert, S. D., Kollmeier, B., & Brand, T. (2014). Prediction of consonant recognition in quiet for listeners with normal and impaired hearing using an auditory model. *Journal of the Acoustical Society of America*, 135(3), 1506–1517.

Lopez-Poveda, E. A. & Meddis, R. (2001). A human nonlinear cochlear filterbank. *Journal of the Acoustical Society of America*, 110(6), 3107–3118.

Laneau, J., Wouters, J., & Moonen, M. (2006). Improved music perception with explicit pitch coding in cochlear implants. *Audiology and Neurotology*, 11(1), 38–52.

Lecluyse, W., Tan, C. M., McFerran, D., & Meddis, R. (2013). Acquisition of auditory profiles for good and impaired hearing. *International Journal of Audiology*, 52(9), 596–605.

Levitt, H. (1971). Transformed up-down methods in psycho-acoustics. *Journal of the Acoustical Society of America*, 49(2 Suppl 2), 467–477.

Litvak, L. M., Spahr, A. J., Saoji, A. A., & Fridman, G. Y. (2007). Relationship between perception of spectral ripple and speech recognition in cochlear implant and vocoder listeners. *The Journal of the Acoustical Society of America*, 122(2), 982–991.

Meddis, R., Clark, N. R., Lecluyse, W., & Jürgens, T. (2013). BioAid—Ein biologisch inspiriertes Hörgerät [BioAid—A biologically inspired hearing]. *Zeitschrift der Audiologie/ Audiological Acoustics*, 52(4), 148–152.

Moore, B. C. J. (1978). Psychophysical tuning curves measured in simultaneous and forward masking. *Journal of the Acoustical Society of America*, 63(2), 524–532.

Moore, B. C. J., Glasberg, B. R., & Roberts, B. (1984). Refining the measurement of psychophysical tuning curves. *Journal of the Acoustical Society of America*, 76(4), 1057–1066.

Nelson, D. A. (1991). High-level psychophysical tuning curves: Forward masking in normal-hearing and hearing-impaired listeners. *Journal of Speech and Hearing Research*, 34(6), 1233–1249.

Nelson, D. A., Donaldson, G. S., & Kreft, H. (2008). Forward-masked spatial tuning curves in cochlear implant users. *The Journal of the Acoustical Society of America*, 123, 1522–1543.

Nelson, D., Kreft, H. A., Anderson, E. S., & Donaldson, G. S. (2011). Spatial tuning curves from apical, middle, and basal electrodes in cochlear implant users. *Journal of the Acoustical Society of America*, 129(6), 3916–3933.

Nelson, D. A., Schroder, A. C., & Wojtczak, M. (2001). A new procedure for measuring peripheral compression in normal-hearing and hearing-impaired listeners. *Journal of Speech and Hearing Research*, 110(6), 2045–2064.

Nogueira, W., Büchner, A., Lenarz, T., & Edler, B. (2005). A psychoacoustic 'NofM'-type speech coding strategy for cochlear implants. *EURASIP Journal on Applied Signal Processing*, 2005, 3044–3059.

Nogueira, W., Rode, T., & Büchner, A. (2016). Spectral contrast enhancement improves speech intelligibility in noise for cochlear implants. *The Journal of the Acoustical Society of America*, 139(2), 728–739.

Oxenham, A. J., & Kreft, H. A. (2014). Speech perception in tones and noise via cochlear implants reveals influence of spectral resolution on temporal processing. *Trends in Hearing*, 18, 1–14.

Oxenham, A. J., & Plack, C. J. (1997). A behavioral measure of basilar-membrane nonlinearity in listeners with normal and impaired hearing. *Journal of the Acoustical Society of America*, 101(6), 1788–1803.

Oxenham, A. J., Simonson, A. M., Turicchia, L., & Sarpeshkar, R. (2007). Evaluation of companding-based spectral enhancement using simulated cochlear-implant processing. *The Journal of the Acoustical Society of America*, 121(3), 1709–1716.

Patterson, R. D., Nimmo-Smith, I., Weber, D. L., & Milroy, R. (1982). The deterioration of hearing with age: Frequency selectivity, the critical ratio, the audiogram, and speech threshold. *Journal of the Acoustical Society of America*, 72(6), 1788–1803.

Plack, C. J., Drga, V., & Lopez-Poveda, E. A. (2004). Inferred basilar-membrane response functions for listeners with mild to moderate sensorineural hearing loss. *Journal of the Acoustical Society of America*, 115, 1684–1695.

Plomp, R. (1988). The negative effect of amplitude compression in multichannel hearing aids in the light of the modulation-transfer function. *Journal of the Acoustical Society of America*, 83, 2322–2327.

Ruggero, M. A., Rich, N. C., Recio, A., Narayan, S. S., & Robles, L. (1997). Basilar-membrane responses to tones at the base of the chinchilla cochlea. *Journal of the Acoustical Society of America*, 101, 2151–2163.

Russell, I. J., & Murugasu, E. (1997). Medial efferent inhibition suppresses basilar membrane responses to near characteristic frequency tones of moderate to high intensities. *Journal of the Acoustical Society of America*, 102(3), 1734–1738.

Shannon, R. V., Zeng, F.-G., Kamath, V., Wygonski, J., & Ekelid, M. (1995). Speech recognition with primarily temporal cues. *Science*, 270, 303–304.

Wouter, J., McDermott, H. J. & Francart, T. (2015). Sound Coding in Cochlear Implants: From electric pulses to hearing. *IEEE Signal Processing Magazine*, 32(2), 67–80.

Weber, D. L. (1977). Growth of masking and the auditory filter. *Journal of the Acoustical Society of America*, 62(2), 424–429.

Williges, B., Dietz, M., Hohmann, V. & Jürgens, T. (2015). Spatial Release From Masking in Simulated Cochlear Implant Users With and Without Access to Low-Frequency Acoustic Hearing. *Trends in Hearing*, 19(1–4), 1–14.

Whitmal, N. A. III, Poissant, S. F., Freyman, R. L., & Helfer, K. S. (2007). Speech intelligibility in cochlear implant simulations: Effects of carrier type, interfering noise, and subject experience. *Journal of the Acoustical Society of America*, 122(4), 2376–2388.

Zhu, Z., Tang, Q., Zeng, F.-G., Guan, T., & Ye, D. (2012). Cochlear-implant spatial selectivity with monopolar, bipolar and tripolar stimulation. *Hearing Research*, 283(1–2), 45–58.